Recent Results from K2K

M. Yokoyama for the K2K Collaboration
Department of Physics, Graduate School of Science, Kyoto University, Kyoto, Japan, 606-8502

The KEK to Kamioka (K2K) long-baseline neutrino oscillation experiment is the first accelerator experiment with baseline greater than 100 km. Its primary goal is the confirmation of the neutrino oscillation observed by Super-Kamiokande collaboration in atmospheric neutrino. Based on data corresponding to 8.9×10^{19}protons on target taken during 1999–2004, we report an evidence of neutrino oscillation with significance of 4.0σ. In total, 107 events are observed with 150.9 expected in the case of no neutrino oscillation. A distortion in neutrino energy spectrum has been also observed. We present an overview of the experiment, analysis procedure, results, and future prospects including the plan for the next generation experiment in Japan, T2K.

1. Introduction

The KEK to Kamioka (K2K) neutrino oscillation experiment [1] is the first accelerator-based experiment with more than 100 km baseline and started data taking in 1999. The primary goal of this experiment is the confirmation of $\nu_\mu \to \nu_x (x = \tau$ or sterile) neutrino oscillation, which was first reported by Super-Kamiokande collaboration with atmospheric neutrino data [2], using artificially produced neutrino beam. Another important goal is search for $\nu_\mu \to \nu_e$ oscillation, which is related to unknown mixing parameter θ_{13}. In addition, improvement of the knowledge about neutrino interactions in a few GeV region is expected using near detectors.

In this article, we present the latest results of K2K experiment based on 8.9×10^{19} protons on target (POT) taken during 1999-2004, putting an emphasis on the improved result of $\nu_\mu \to \nu_x$ oscillation measurement. Future prospect of the experiment, including plan for the next generation neutrino oscillation experiment in Japan, is also presented.

2. K2K Experiment

Figure 1 shows a schematic picture of the K2K experiment. Almost ($\simeq$98%) pure ν_μ beam with a mean energy of 1.3 GeV is produced by 12 GeV proton synchrotron at High Energy Accelerator Research Organization (KEK) in Tsukuba, Japan. Properties of neutrino beam are measured at two points 250 km apart, with near detector (ND) system at KEK and with Super-Kamiokande. Comparing these two measurements, we study neutrino oscillation.

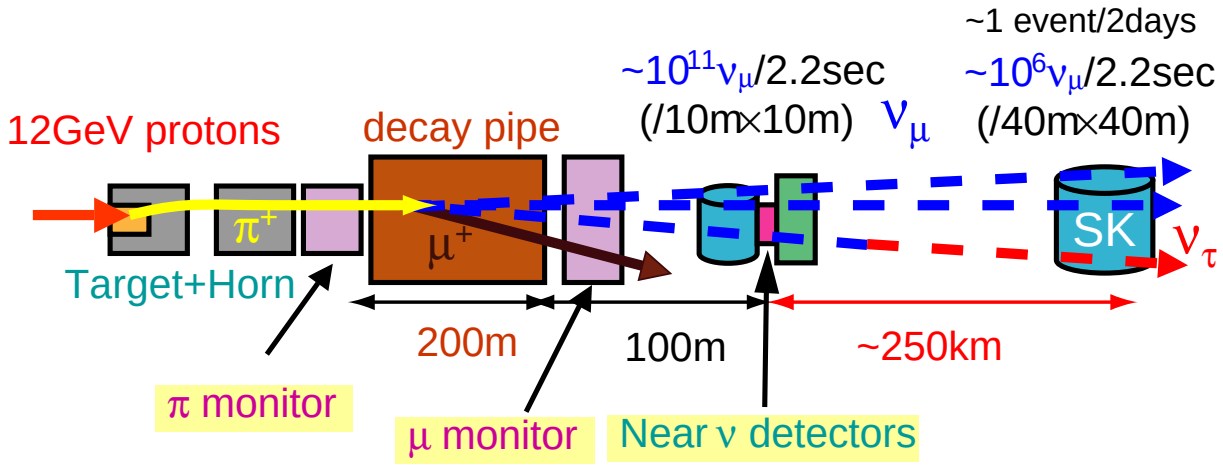

Figure 1: Schematic drawing of K2K experiment.

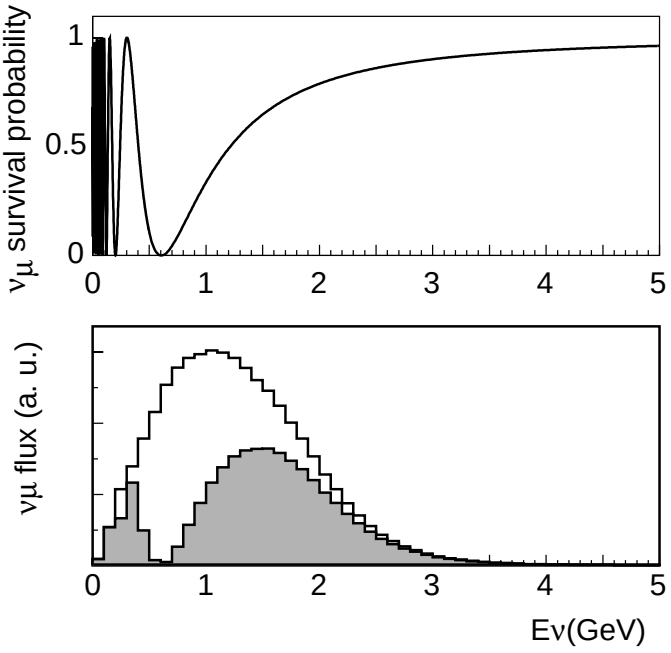

Figure 2: Top: survival probability of muon neutrino as a function of neutrino energy after oscillation with 250 km baseline. Bottom: expected neutrino energy spectrum with (hatched) and without (open) neutrino oscillation in K2K. The oscillation parameters are set to $\Delta m^2_{23} = 3.0 \times 10^{-3}$ and $\sin^2 2\theta_{23} = 1.0$.

If there was neutrino oscillation, the survival probability of muon neutrino with energy E_ν (GeV) after traveling distance L (km) is written under the assumption of oscillation between two flavors as

$$P(\nu_\mu \to \nu_\mu) = 1 - \sin^2 2\theta_{23} \sin^2 \left(\frac{1.27 \times \Delta m^2_{23} \times E_\nu(\mathrm{GeV})}{L(\mathrm{km})} \right),$$

where θ_{23} and Δm^2_{23} are the mixing angle and mass-squared difference between second and third generation neutrinos, respectively. Figure 2 shows the survival probability ($P(\nu_\mu \to \nu_\mu)$, top) and expected neutrino spectrum at SK (bottom, open: without ν oscillation, hatched: with oscillation) in K2K. Here, $\Delta m^2_{23} = 3.0 \times 10^{-3}$ and $\sin^2 2\theta_{23} = 1.0$ are used as oscillation parameters. Since our beam energy is well below the production threshold of τ lepton, the charged current interaction does not happen for oscillated neutrino and we observe a "disappearance" of neutrino events as the consequence of neutrino oscillation. In K2K, because the distance L is fixed at the baseline of experiment (250 km), the neutrino oscillation manifests itself as a distortion of neutrino energy spectrum as well as reduction of muon neutrino flux. In the rest of this section, experimental setup used in K2K is described.

2.1. K2K Neutrino Beamline

A schematic drawing of the K2K beamline is shown in Fig. 3. A neutrino beam is produced using 12 GeV proton synchrotron at KEK. About 6×10^{12} protons are extracted from the accelerator within 1.1 μsec, every 2.2 seconds. Protons hit an aluminum target and produce secondary particles, mainly pions. Positively charged particles are focused by two magnetic horns, which increases the neutrino flux by a factor of twenty. Then, neutrinos are produced from decays of pions: $\pi^+ \to \mu^+ + \nu_\mu$ in a 200m-long decay volume.

Primary protons are monitored using current transformer (CT) and segmented plate ion chamber (SPIC). CT is used to estimate the number of protons delivered to the target, while SPIC is used to monitor the spacial profile of the proton beam. Figure 4 shows the accumulated POT delivered from KEK-PS and the average number of protons per pulse as a function of time.

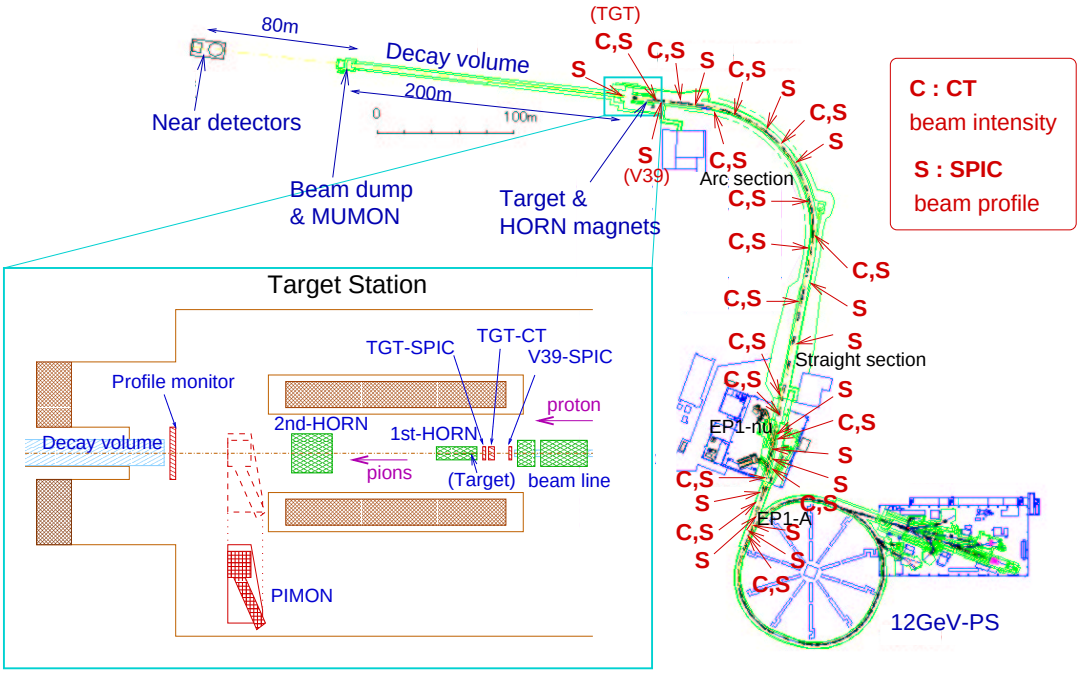

Figure 3: A schematic drawing of the K2K beamline.

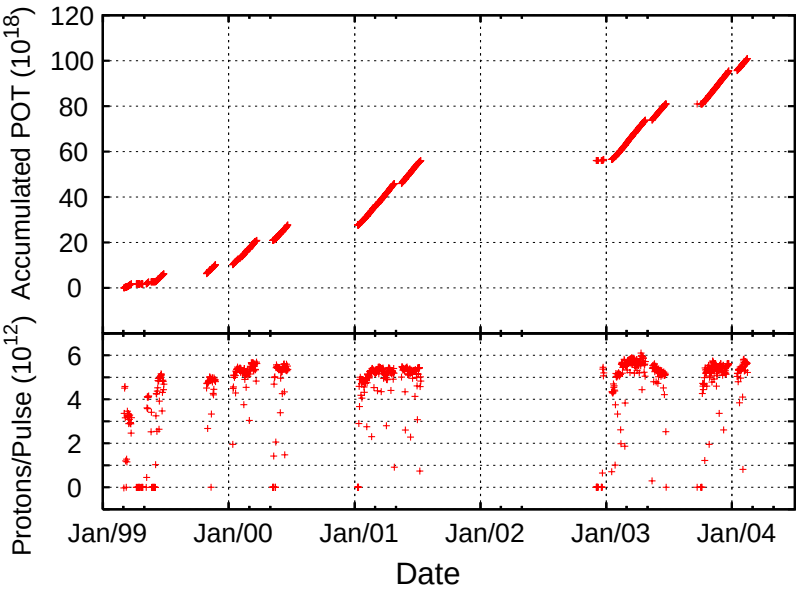

Figure 4: Integrated POT delivered from KEK-PS (top) and average number of protons per pulse (bottom) as a function of time.

The kinematics of secondary pions just before the decay volume were measured using a specially-designed gas Čerencov counter (pion monitor, PIMON) in the early stage of the experiment. The main purpose of PIMON is to estimate the difference of neutrino spectrum seen by near and far detectors, originating from the finite size of the neutrino production point. In K2K, this difference is corrected using the energy-dependent ratio of far to near neutrino flux, which can be calculated once the momentum and the angular distributions of pions are known. In order to be insensitive to the 12 GeV primary protons, PIMON has sensitivity to only pions with momentum greater than

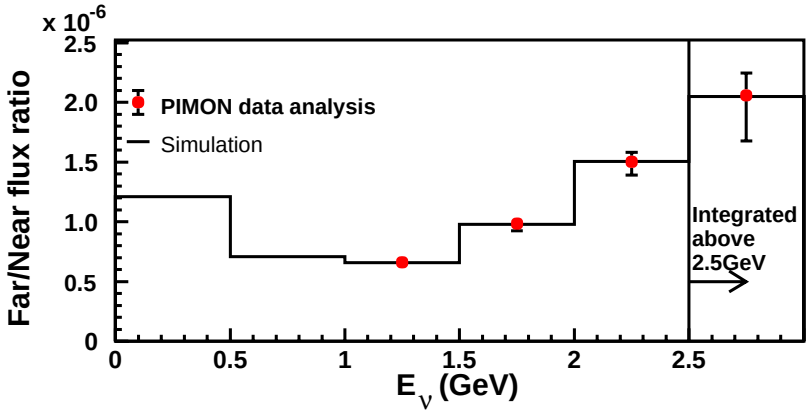

Figure 5: Flux ratio between the near and far detectors for each neutrino energy. Points with error bars represent measurement result with PIMON. Histogram shows result of beam Monte Carlo simulation.

2 GeV, corresponding to the neutrino energy greater than 1 GeV. Because the measurement with PIMON agreed well with our Monte Carlo (MC) simulation, we use MC simulation to calculate the center value of the F/N ratio. We estimated uncertainty of the F/N ratio from PIMON measurement for neutrino energy above 1 GeV and from model dependence of pion production below 1 GeV.

In order to monitor the intensity, profile and direction of the neutrino beam spill by spill, muon monitor (MUMON) system is installed just after the beam dump. MUMON consists of a segmented ionization chamber and an array of silicon pad detectors. It measures muons which are produced from decays of pions, $\pi^+ \to \mu^+\nu_\mu$, together with neutrinos. Placed behind the beam dump, 3.5 m iron and 2 m concrete, to avoid hadron background, it is sensitive only to muons with momentum greater than 5.5 GeV/c. Figure 6 shows the stability of beam direction monitored by MUMON. Throughout the experiment period, the beam direction was stable within 1 mrad, while < 3 mrad is the required precision of the directional control to keep the systematic effect on the neutrino spectrum and flux at SK negligible.

In order to assure the quality of data used in the analysis, we use only spills for which we confirm good beam condition. Spills with poor quality, such as low proton intensity, low horn current, abnormal condition in beamline monitors, are removed from data set.

2.2. Near Detector System

The near detector system is located about 300 m downstream from the pion production target to measure the neutrino beam flux and spectrum just after production. Figure 7 shows a schematic drawing of K2K ND system as of year 2004. ND consists of two detector systems; a one-kiloton water Čerenkov detector (1KT) and fine-grained detector system (FGD). From 1999 to 2001, FDG was comprised of a scintillator fiber tracker with water target (SciFi), a lead glass calorimeter (LG), and a muon range detector (MRD). In this period (called K2K-I), 4.8 $\times 10^{19}$ POT was accumulated. From January 2003 to June 2003, 2.3×10^{19} POT was taken without LG (K2K-IIa). In the summer 2003, a fully-active scintillator detector (SciBar) was installed in place of LG and 1.9 $\times 10^{19}$ POT was recorded (K2K-IIb).

The 1KT has 680 20-inch photomultiplier tubes (PMTs) on a 70 cm grid lining a 8.6m diameter, 8.6m high cylinder. It uses the same technology and analysis algorithms as used in the SK. The PMTs themselves and their arrangement are the same as in SK, giving the same fractional coverage by photo-cathode (40%) as SK-I. It has 4π coverage and good reconstruction efficiency for muons with momentum below 1 GeV/c. However, the 1KT has little reconstruction efficiency of muon momentum above 1.5 GeV/c because muons exit the detector.

The SciFi detector [3] consists of 20 layers of scintillating fiber sheets interleaved with water target tanks. Each tracking layer is made of two scintillating fiber sheets to provide two dimensional position. The water target is

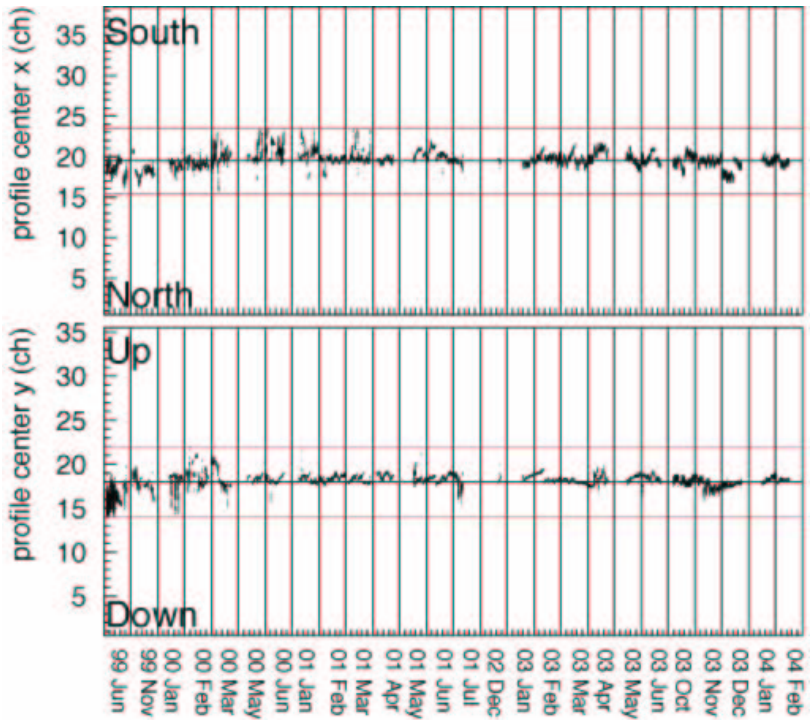

Figure 6: Beam direction monitored by MUMON. Top: horizontal direction, bottom: vertical direction. The horizontal lines represents the direction of SK (black) and ±1 mrad deviations (red).

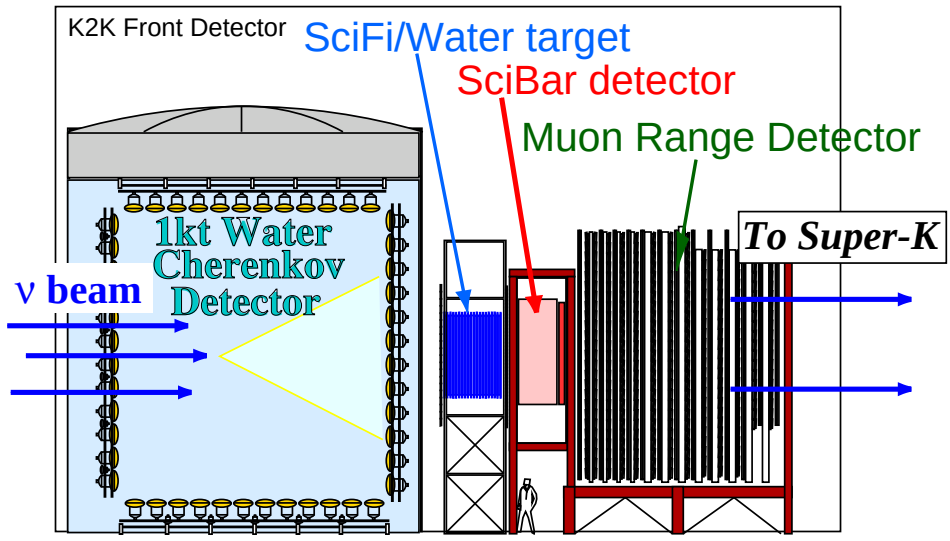

Figure 7: Schematic drawing of ND system in K2K-IIb period. In K2K-I, a lead glass calorimeter was located in the place of SciBar.

contained in a 6 cm wide aluminum tank with 0.18 cm wall thickness. The light from scintillator is read out using 24 set of image intensifier tubes and CCD cameras. The fiducial mass of the SciFi detector is 5.9 tons.

The LG was used to measure ν_e contamination in the neutrino beam. It consists of 10 modules, each module in turn consists of 60 cells of lead glass reused from TOPAZ experiment at TORISTAN.

The SciBar detector [4] has constructed to upgrade the FGD system, replacing the LG after the measurement of ν_e contamination was done. It consists of 14,448 extruded plastic scintillator bars with dimensions of 1.3 × 2.5 ×

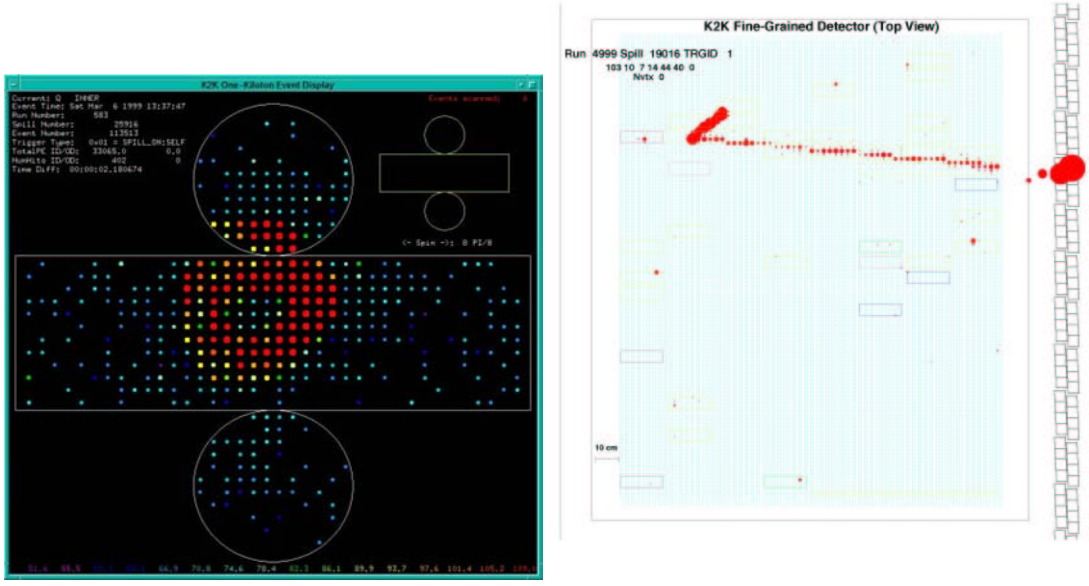

Figure 8: Displays of neutrino events recorded with 1KT (left) and SciBar (right) detectors.

300 cm^3, arranged in 64 layers. The total size and mass are about 300 × 300 × 170 cm^3 and 15 tons, respectively, out of which 9.38 tons is used as a fiducial volume. The light from scintillators are read out by wavelength shifting fibers and multi-anode photomultipliers. Having almost no dead region and fine segmentation, SciBar can detect all charged particles produced in neutrino interactions with high efficiency.

The MRD [5] consists of 12 iron absorbers sandwiched with 13 sets of drift tubes. The total mass of iron plates is 915 tons, giving large number of neutrino interactions to monitor the stability of the intensity, profile and spectrum of the neutrino beam. The MRD also provide momentum measurement for muons produced in fine-grained detectors in upstream (SciFi and SciBar).

In order to reach the MRD, muons need to have momentum greater than ∼0.5 GeV. Therefore, the momentum acceptance of FGD in spectrum measurement is in higher region than that of 1KT. The 1KT and FGD have different detector systematics and acceptance, giving us complementary information about neutrino beam property and neutrino-nucleus interaction.

Figure 8 shows displays of typical neutrino events recorded by 1KT and SciBar detectors.

2.3. Far Detector

We use the Super-Kamiokande (SK) [6, 7], a fifty kiloton water Čerencov detector, as the far detector. From 1999 to 2001, the inner detector surface of SK had 11,146 20-inch photo-multiplier tubes covering 40% of the total area (SK-I, which is used for K2K-I period). Starting from January 2003 (SK-II, corresponding to K2K-II), 19% of the SK inner detector is covered using 5182 PMTs, each enclosed in a fiber reinforced plastic shell with an acrylic cover. The transparency and reflection of these covers in water are 97% and 1% respectively.

The charged particle is reconstructed using the timing and charge information of Čerenkov light detected by PMTs. Muons (or MIP particle) and electrons (and converted gammas) are separated using the pattern of Čerenkov ring. A Čerenkov ring produced by an electron is diffused by its electromagnetic shower and multiple scattering, while that produced by a muon has a clear edge, and a low energy muon has a smaller opening angle than an electron.

2.4. Neutrino Interaction Models

Neutrino interactions are simulated by the NEUT program library [8]. Charged-current quasi-elastic scattering (CCQE) is simulated based on the Llewellyn Smith's model [9]. The Rein and Sehgal's model [10] is used to simulate single meson production mediated by a baryon resonance. The axial vector mass, M_A, is set to $1.1\,\mathrm{GeV}/c^2$ for both CCQE and the single pion production models. Coherent pion production is simulated using the model of Rein and Sehgal [11] with modified cross section according to Marteau et al. [12]. For deep inelastic scattering, GRV94 nucleon structure function [13] with a correction by Bodek and Yang [14] is adopted to calculate the cross section.

3. Near Detector Measurements

Using the near detector system, we measure the total number of neutrino interactions and the neutrino energy spectrum. These are indispensable to look for signatures of neutrino oscillation, i.e. reduction of the event and distortion of the energy spectrum. In addition, based on a large data sample collected at the near detectors, we study neutrino-nucleus interaction, which is also important for the measurement of neutrino oscillation with small uncertainty.

3.1. Number of Neutrino Interaction

The number of total neutrino interactions is measured using the 1KT detector, because it uses the same target and detection technique as far detector (SK) and has the smallest systematic error. The events with visible energy greater than ~ 100 MeV are used for this analysis. From the number of observed events inside the fiducial volume ($N^{\mathrm{obs}}_{\mathrm{1KT}}$), the expected number of events at SK in the case of no oscillation ($N^{\mathrm{exp}}_{\mathrm{SK}}$) is estimated as

$$N^{\mathrm{exp}}_{\mathrm{SK}} = N^{\mathrm{obs}}_{\mathrm{1KT}} \times \frac{\int \Phi_{\mathrm{SK}}(E_\nu)\sigma(E_\nu)dE_\nu}{\int \Phi_{\mathrm{1KT}}(E_\nu)\sigma(E_\nu)dE_\nu} \times \frac{M_{\mathrm{SK}}}{M_{\mathrm{1KT}}} \times \frac{\epsilon_{\mathrm{SK}}}{\epsilon_{\mathrm{1KT}}} \tag{1}$$

where $\Phi_i(E_\nu)$, $\sigma(E_\nu)$, M_i, and ϵ_i (i=SK, 1KT) represents the flux, cross-section, fiducial mass and efficiency, respectively. The second term in the right hand side of Eq. 1 is calculated from the far/near spectrum ratio shown in Fig. 5 and the neutrino energy spectrum measured in the near detector (described in Sec. 3.2). The cross-section cancels because the target is the same. The efficiency of 1KT, SK-I and SK-II is 74.5%, 77.0% and 78.2%, respectively. The expected number of fully contained events at SK without oscillation is

$$N^{\mathrm{exp}}_{\mathrm{SK}} = 151^{+12}_{-10}(\mathrm{syst}).$$

The major contributions to the errors come from the uncertainties in the far to near ratio (5.1%) and the normalization (5.1%); the latter is dominated by the uncertainty in the fiducial volumes due to the vertex reconstruction at both 1KT and SK.

3.2. Neutrino Energy Spectrum

The neutrino energy spectrum at the near detector system is measured by 1KT, SciFi and SciBar. Assuming the CCQE interaction and neglecting Fermi momentum, the neutrino energy can be reconstructed using the muon momentum alone as

$$E^{\mathrm{rec}}_\nu = \frac{(m_N - V)E_\mu - m_\mu^2/2 + m_N V - V^2/2}{(m_N - V) - E_\mu + p_\mu \cos\theta_\mu},$$

where m_N, V, E_μ, m_μ, p_μ and θ_μ are the nucleon mass, the nuclear binding potential ($V = 27$ MeV), muon energy, mass, momentum and angle with respect to the neutrino beam direction, respectively.

Table I: Charged current quasi-elastic (CCQE) efficiency and purity for each sub-sample used in the spectrum analysis. Values without parentheses represent CCQE reconstruction efficiency [%] out of all CCQE events in the fiducial volume, and values within parentheses represent CCQE purity [%] for each sub-sample.

	1-track or	2-track		Total
	1-ring μ like	QE	non-QE	
1KT	53 (59)	—	—	53
SciFi I	39 (50)	5 (53)	2 (11)	46
SciFi IIa	36 (57)	5 (58)	2 (12)	42
SciBar	51 (57)	15 (72)	4 (17)	70
SK	86 (58)	—	—	86

We use two dimensional information of p_μ and θ_μ rather than $E_\nu^{\rm rec}$ itself to measure the neutrino spectrum. The distributions of p_μ and θ_μ are compared with MC expectation using a χ^2 fitting method, treating the neutrino energy spectrum in MC as fitting parameters. In order to suppress uncertainty from neutrino interaction model, we introduce a parameter to correct the relative cross section of CCQE and non-QE interactions ($R_{\rm nqe}$). By simultaneously fitting all data from different detectors and different kinematics samples, we can obtain neutrino energy spectrum in a broad range and check the consistency of whole analysis.

3.2.1. Event Selection

For 1KT, we use events with only one muon-like Čerenkov ring reconstructed. Because most of protons from CCQE interaction has momentum below Čerenkov threshold (1.07 GeV/c), this type of events is the purest sample of CCQE in water Čerenkov detectors.

For SciFi and SciBar, we use events in which one or two track are reconstructed. At least one of tracks is required to be consistent with muon, by selecting track which penetrates into LG (SciFi in K2K-I) or MRD (SciFi K2K-IIa and SciBar). For two-track events, we use kinematic information to discriminate between CCQE and non-QE interactions. The direction of the recoil proton can be predicted from p_μ and θ_μ assuming a CCQE interaction. If the difference between the observed and the predicted direction of the second track is within 25 degrees, the event is in the QE enriched sample. Events for which this difference is more than 30 degrees for SciFi and 25 degrees for SciBar are put into the non-QE sample. The QE efficiency and purity of each sample is estimated from the MC simulation and are summarized in Tab. I.

3.2.2. Spectrum Measurement

We measure the neutrino energy spectrum at the near detectors by fitting the two-dimensional distributions of muon momentum (p_μ) versus angle with respect to the beam direction (θ_μ). Seven event categories (one for 1KT and three for each of SciFi and SciBar) are simultaneously fitted. A χ^2 fitting method is employed to compare the data and the MC expectation. The neutrino flux is divided into eight energy bins; $(0-0.5)$, $(0.5-0.75)$, $(0.75-1.0)$, $(1.0-1.5)$, $(1.5-2.0)$, $(2.0-2.5)$, $(2.5-3.0)$, and (>3.0) GeV. For each category and each neutrino energy bin, we make a template of p_μ versus θ_μ distribution based on the MC simulation. In addition, separate template is prepared for CCQE and non-QE interactions. An example of p_μ-θ_μ distribution for SciBar one track events is shown in Fig. 9. During the fit, the flux in each energy bin is re-weighted relative to the values in the beam MC and the data are compared with the sum of MC templates. These weights are normalized relative to 1.00 for the $E_\nu = 1.0-1.5$ GeV bin. An overall normalization is included as a free parameter in the fit. The parameter $R_{\rm nqe}$ is used to re-weight the ratio between the QE and non-QE cross-section relative to the MC simulation. The systematic uncertainties of the near detectors, e.g. the energy scales, the track finding efficiencies, are incorporated into the fitting parameters. For SciBar, possible differences of target material and the nuclear effect are studied and included as a systematic uncertainty. In addition, the spectrum measurement by PIMON is used as a constraint on the re-weighting factors.

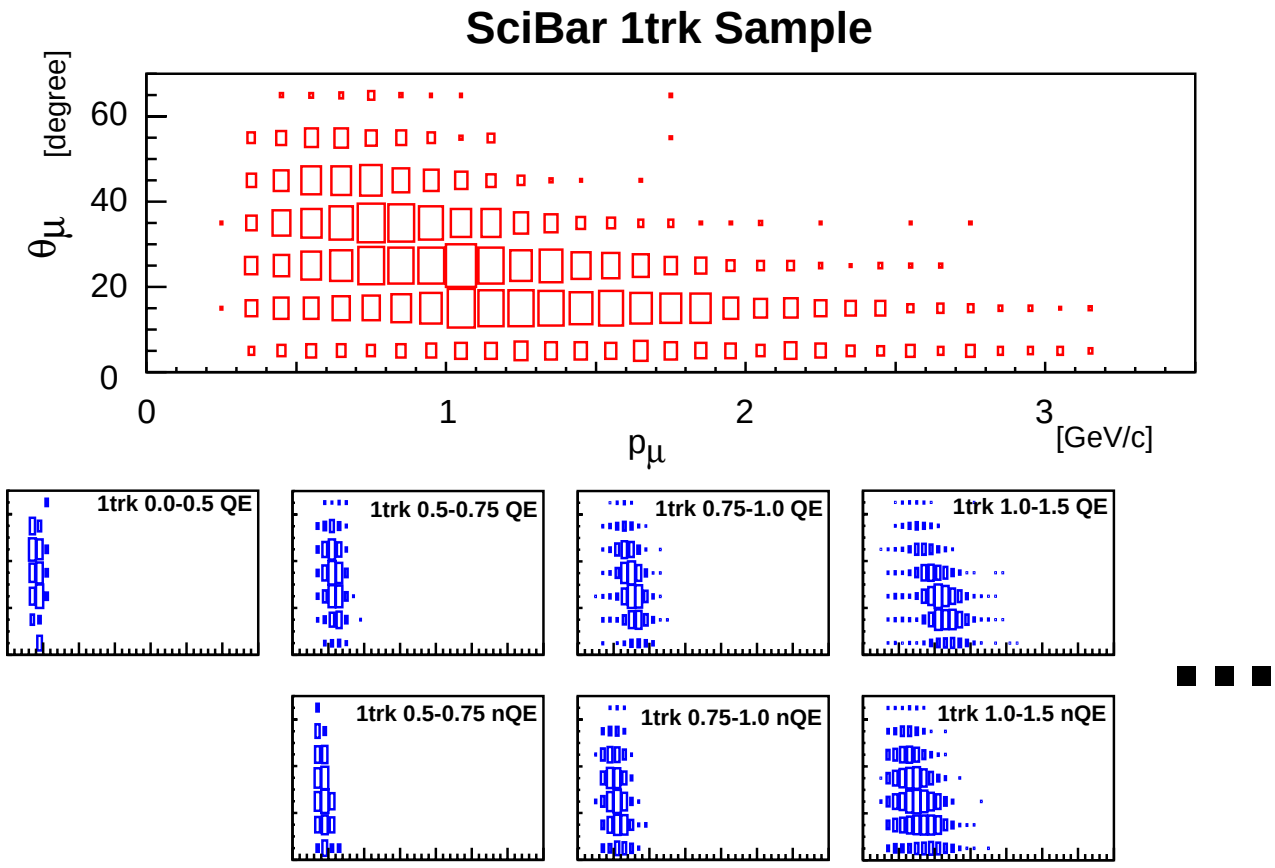

Figure 9: Distribution of p_μ versus θ_μ for SciBar one track events. Top: real data. Bottom: part of MC templates.

In order for this fitting method to correctly work, it is essential that we understand the neutrino interaction well. However, we observe a significant deficit of forward going muons in all near detector data compared to the MC simulation, which can not be explained by adjusting the parameters of neutrino interaction models and/or the neutrino spectrum. To avoid any possible bias due to this, we perform the fit using only data with $\theta_\mu > 20(10)$ degrees for 1KT (SciFi and SciBar). The χ^2 value at the best fit is 538.5 for 479 degrees of freedom (DOF). The resulting E_ν spectrum and its error are summarized in Tab. II and shown in Fig. 10. The best fit value of $R_{\rm nqe}$ is 0.95.

3.2.3. Correction of Neutrino Interaction Model

Although the energy spectrum can be measured with partial data, we need to modify the MC models to account for the observed deficit in order to use all data in SK. Muons in the forward direction also correspond to events with a low value for the square of the momentum transfer (q^2), the relevant parameter in the neutrino interaction models. From inspection of all subsamples, the amount of resonant pion production and coherent pion production at low q^2 in the MC simulation are possible sources of the forward muon deficit. Figure 11 shows the distributions of q^2 reconstructed assuming CCQE interaction ($q^2_{\rm rec}$) for SciFi and SciBar two track non-QE enriched samples.. We modify the MC simulation used in the near and the far detector analysis to account for the effect of the observed deficit. For resonant pions, we suppress the cross section by q^2/A for $q^2 < A$ and leave it unchanged for $q^2 > A$. From a fit to the SciBar 2-track non-QE sample, A is 0.10 ± 0.03 (GeV/c)^2. Alternatively, if we assume that the source is coherent pion production, we find the observed distribution is reproduced best with zero coherent pion after trying several suppression functions.

Table II: E_ν spectrum fit results. $\Phi_{\rm ND}$ is the best fit value of flux for each E_ν bin. It is given relative to the 1.0–1.5 GeV bin. The percentages of uncertainties in $\Phi_{\rm ND}$, far/near (F/N) ratio, and reconstruction efficiencies of SK-I and SK-II are also shown.

E_ν (GeV)	$\Phi_{\rm ND}$	$\Delta(\Phi_{\rm ND})$	Δ(F/N)	$\Delta(\epsilon_{\rm SK\text{-}I})$	$\Delta(\epsilon_{\rm SK\text{-}II})$
0.0 – 0.5	0.032	46	2.6	3.7	4.5
0.5 – 0.75	0.32	8.5	4.3	3.0	3.2
0.75 – 1.0	0.73	5.8	4.3	3.0	3.2
1.0 – 1.5	$\equiv 1$	—	4.9	3.3	8.2
1.5 – 2.0	0.69	4.9	10	4.9	7.8
2.0 – 2.5	0.34	6.0	11	4.9	7.4
2.5 – 3.0	0.12	13	12	4.9	7.4
3.0 –	0.049	17	12	4.9	7.4

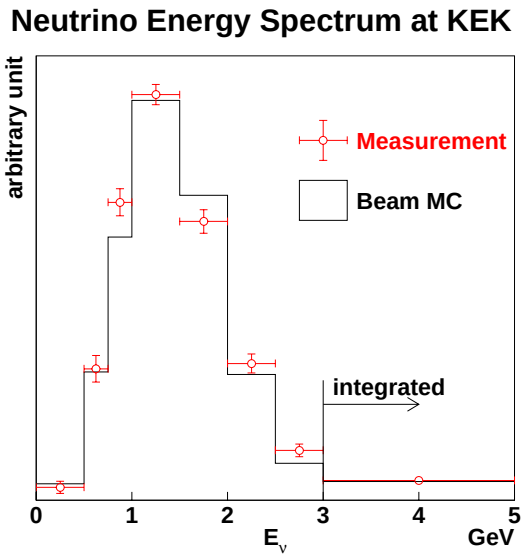

Figure 10: Measured neutrino energy spectrum at near detector site.

Considering both possibilities mentioned above, we check if the p_μ-θ_μ distributions can be reproduced with modified MC model. The E_ν spectrum is kept fixed at the values already obtained in the first step, but now we use data at all angles. The best fit value for $R_{\rm nqe}$ is 1.02 (1.06) with χ^2/DOF of 638.1/609 (667.1/606) when we suppress resonant pion (eliminate the coherent pion). The p_μ and θ_μ distributions from all detectors are well reproduced for both cases with reasonable χ^2, including the small θ_μ region. The adopted corrections are validated by the fact that the correction determined by SciBar two track non-QE sub-sample is compatible with all the other samples. Some of p_μ and θ_μ distributions after correction to the MC simulation are shown in Fig. 12. If we repeat the fit with the E_ν spectrum free, the results are still consistent with the first step. Examining these results carefully, we conclude that we cannot identify which is the source of the observed deficit in the low q^2 region. Because the value of $R_{\rm nqe}$ changes depending on the choice of model, an additional systematic error of 0.1 is assigned to $R_{\rm nqe}$. For the oscillation analysis presented in this letter, we choose to suppress the resonance production mode in the MC simulation and when we determine the central value of $R_{\rm nqe}$. However, we find that the final oscillation results and allowed regions do not change if we instead choose to eliminate coherent pion, or use our MC without any corrections.

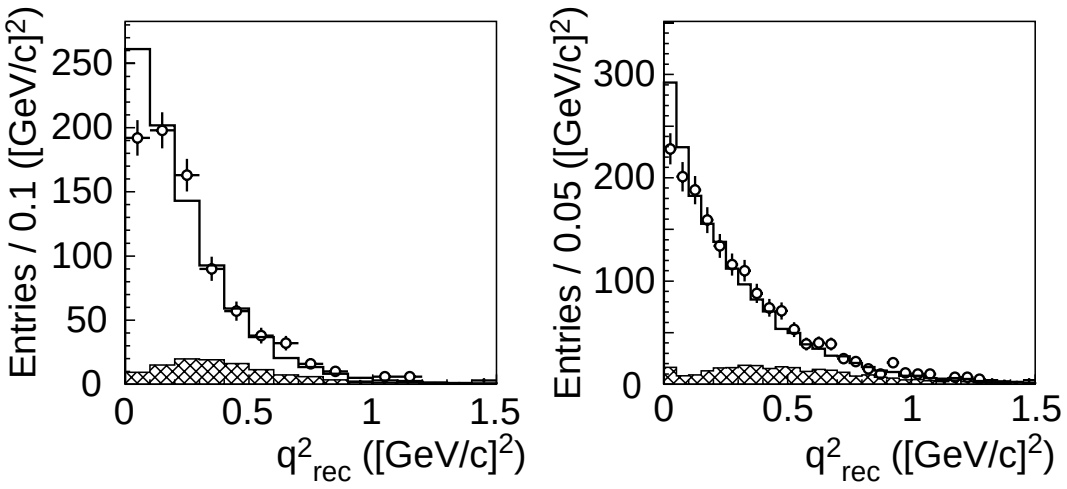

Figure 11: Reconstructed q^2 distributions for 2-track nonQE-enriched samples of SciFi (left) and SciBar (right). Open circles with error bars are data, solid lines are MC predictions before correction of low q^2 part, and hatched areas show CC-QE component estimated from MC simulation. A clear deficit is observed in the low q^2 region.

Table III: The SK event summary. MC is a prediction by the MC simulation without neutrino oscillation.

K2K-I+II	Data	MC
1-ring μ-like	57	85.5
1-ring e-like	10	8.7
multi-ring	40	56.7
total	107	150.9

4. Super-K Observation and Oscillation Analysis

4.1. Event Selection and Reconstruction in SK

Neutrino interactions at SK are selected based on the time difference between the beam spill start and the event trigger. The timing is synchronized using the global positioning system (GPS). The time difference, after subtracting the time of flight for 250 km baseline, should be distributed around the interval from 0 to 1.1μs to match the width of the beam spill of the KEK-PS. Since the measured uncertainty of the synchronization accuracy for the two sites is less then 200 nsec, beam-induced events are selected in a 1.5 μsec window. Neutrino events fully contained (FC) in the SK detector are selected by requiring that there is no activity in the outer detector and that the energy deposit in the inner detector is greater than 30 MeV. Events with reconstructed vertices inside 22.5 kiloton fiducial volume are used for the analysis.

Figure 13 shows the timing difference distribution of events recorded by SK at each step of selection. A clear peak in time with the neutrino beam from the KEK-PS is observed in the analysis time window. Figure 14 shows the distribution of the event timing after correcting the time of flight in the detector. The bunch structure of K2K-PS is clearly seen. One hundred and seven FC events are observed in the fiducial volume, while the 1.5 μsec selection window gives an expected background of 2×10^{-3} events from atmospheric neutrino interactions. A summary of events observed in SK is shown in Tab. III with MC expectation in the case of no oscillation.

We reconstruct the neutrino energy ($E_\nu^{\rm rec}$), assuming CC-QE kinematics, from p_μ and θ_μ for the 57 events in the 1-ring μ-like subset of the SK data. The detector systematics of SK-I and SK-II are slightly different because of the change in the number of inner detector PMTs. In the oscillation analysis based on the energy spectrum, the main contribution to the systematic error is the energy scale uncertainty: 2.0% for SK-I and 2.1% for SK-II. Uncertainties

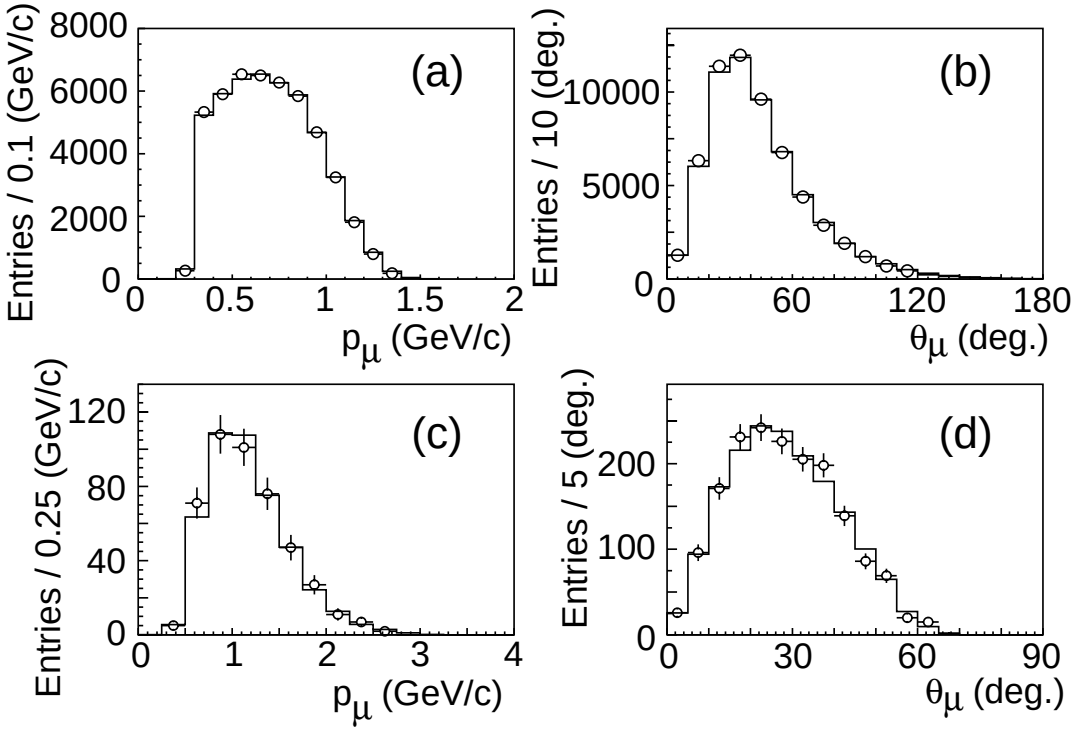

Figure 12: A selection of muon momentum (p_μ) and direction (θ_μ) distributions: (a) the p_μ distribution of 1KT fully contained 1-ring μ-like sample, (b) 1KT θ_μ for the same sample, (c) SciFi p_μ for 2-track QE sample, and (d) SciBar θ_μ for 2-track nonQE sample. Open circles represent data, while histograms are MC predictions using the best fit E_ν spectrum and suppression of the resonant pion production.

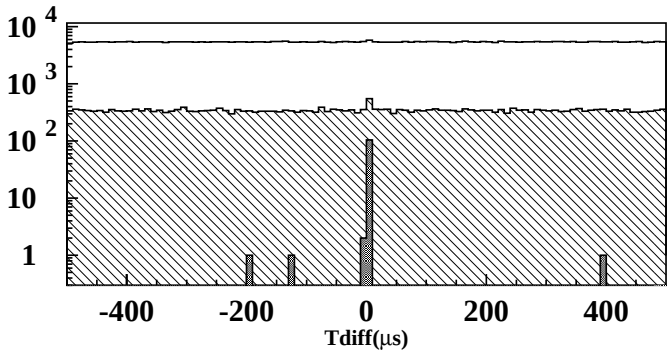

Figure 13: Distribution of timing difference between beam start and event detection after subtracting time of flight for 250 km baseline (ΔT). Open, hatched and filled histograms represent events with $|\Delta T| < 500$ nsec, after requiring > 30 MeV energy deposit in the inner detector, and after all selection except timing, respectively.

for the ring counting and particle identification are estimated using the atmospheric neutrino data sample and MC simulation. The differences between the K2K and atmospheric neutrino fluxes are also taken into account.

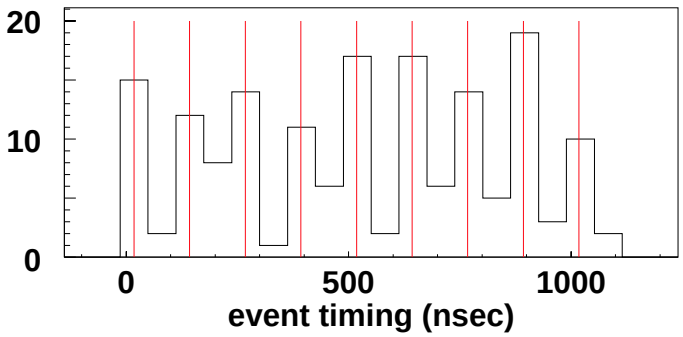

Figure 14: Timing distribution of events selected at SK.

4.2. Oscillation Analysis

4.2.1. Definition of Likelihood

A two-flavor neutrino oscillation analysis, with ν_μ disappearance, is performed using a maximum-likelihood method. The oscillation parameters, $(\sin^2 2\theta, \Delta m^2)$, are estimated by maximizing the product of the likelihood for the observed number of FC events ($\mathcal{L}_{\rm num}$) and that for the $E_\nu^{\rm rec}$ spectrum shape of one ring muon-like events ($\mathcal{L}_{\rm shape}$). We use one hundred and seven events in the estimation of $\mathcal{L}_{\rm num}$, while fifty seven one-ring muon like events are used for $\mathcal{L}_{\rm shape}$. The probability density function (PDF) for $\mathcal{L}_{\rm num}$ is the Poisson probability to observe one hundred and seven events when the expected number of events is $N^{\rm exp}$, where $N^{\rm exp}$ depends on the estimation described in Sec. 3.1, the oscillation parameters and systematic uncertainties. The PDF for $\mathcal{L}_{\rm shape}$ is the expected $E_\nu^{\rm rec}$ distribution at SK, which is estimated from the neutrino energy spectrum measured at near detectors multiplied with the far/near ratio. The response of SK detector is incorporated based on the MC simulation.

The PDFs are defined for K2K-I and K2K-II separately. The systematic uncertainties due to the following sources are taken into account in the PDFs: the E_ν spectrum measured by the near detectors, the far to near ratio, the reconstruction efficiency and absolute energy scale of SK, the ratio of neutral current to charged current QE cross section, the ratio of CC non-QE to CC-QE cross section and the overall normalization. A constraint term ($\mathcal{L}_{\rm syst}$) is multiplied with the likelihood for each of these systematics, and $\mathcal{L}_{\rm num} \times \mathcal{L}_{\rm shape} \times \mathcal{L}_{\rm syst}$ is maximized during the fit. The total number of parameters varied in the fit is thirty-four, including two oscillation parameters.

4.2.2. Fit Results

The best fit point within the physical region is found to be $(\sin^2 2\theta,\ \Delta m^2)=(1.0, 2.8 \times 10^{-3}\ {\rm eV}^2)$. The expected number of events at this point is 103.8, which agrees well with the 107 observed. The best fit E_ν distribution is shown with the data in Fig. 15. The consistency between the observed and fit E_ν distributions is checked using a Kolmogorov-Smirnov (KS) test. For the best fit parameters, the KS probability is 36%, while that for the no-oscillation hypothesis is 0.08%. The highest likelihood is at a point $(1.5, 2.2 \times 10^{-3}\ {\rm eV}^2)$ which is outside of the physical region. The probability that we would get $\sin^2 2\theta \geq 1.5$ if the true parameters are our best fit physical parameters is 13%, based on MC virtual experiments. We refer only to the best fit result inside the physical region. The fit results for all the systematic parameters are reasonable. The fits for the K2K-I and K2K-II sub-samples are consistent with the result for the whole sample.

The possibility that the observations are due to a statistical fluctuation instead of neutrino oscillation is estimated by computing the likelihood ratio of the no-oscillation case to the best fit point. If there is no oscillation, the probability of this result is $0.0050\%(4.0\sigma)$. When only normalization (shape) information is used, the probability is 0.26% (0.74%). Allowed regions for the oscillation parameters are evaluated by calculating the likelihood ratio of each point to the best fit point and are drawn in Fig. 16. The 90% C.L. contour crosses the $\sin^2 2\theta = 1$ axis at

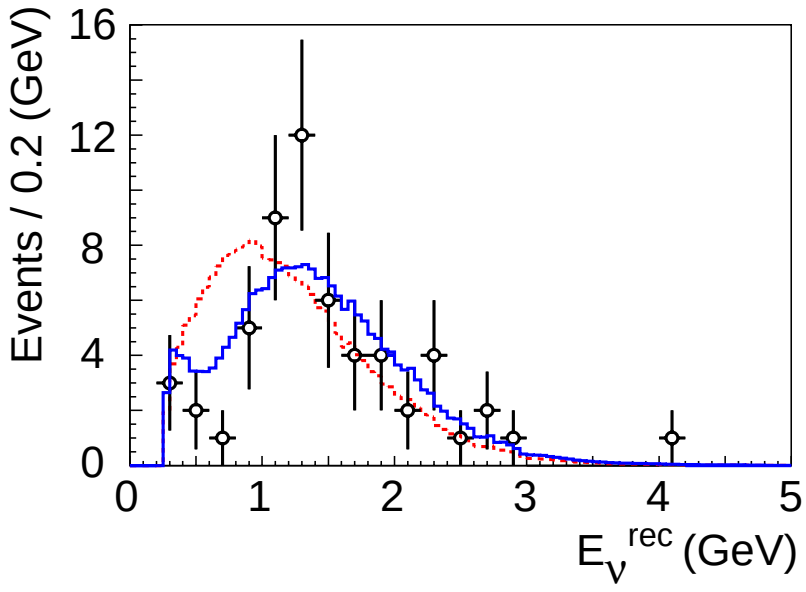

Figure 15: The reconstructed E_ν distribution for the SK 1-ring μ-like sample. Points with error bars are data. The solid line is the best fit spectrum. The dashed line is the expected spectrum without oscillation. These histograms are normalized by the number of events observed (57).

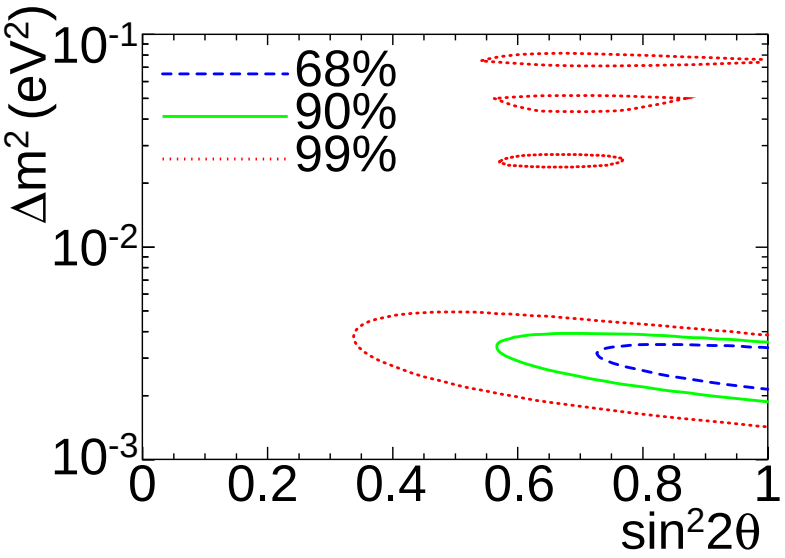

Figure 16: Allowed regions of oscillation parameters. Dashed, solid and dot-dashed lines are 68.4%, 90% and 99% C.L. contours, respectively.

$\Delta m^2 = 1.9$ and 3.6×10^{-3} eV^2. The oscillation parameters from the E_ν spectrum distortion alone, or the total event analysis alone also agree. We conclude that we have observed the neutrino oscillation with 4.0σ significance.

5. Prospects of K2K

5.1. Neutrino Interaction Study

The detailed knowledge of neutrino-nucleus interaction is of great importance for the current and future neutrino oscillation experiments. Using a large sample collected with the near detectors, various studies of neutrino-nucleus interactions are ongoing in K2K. These include, but not limited to:

- Measurement of single π^0 production cross section with 1KT [15]. This channel is expected to be one of the most significant background in the $\nu_\mu \to \nu_e$ appearance search [16, 17].
- Axial vector mass (M_A) measurement for the CCQE interaction with SciFi. M_A is a basic parameter to describe the nucleon form factor, which affects cross section of neutrino-nucleus scattering but never measured with water target in past.
- Study of charged current coherent pion production with SciBar. As presented in this report, this mode is one of candidates for the source of the forward going muon deficit observed in K2K. Using SciBar data, in which pions can be distinguished from protons based on dE/dx, we may measure the charged current coherent pion production.

5.2. Neutrino Oscillation Measurements

Measurements of neutrino oscillation will be updated with more statistics and improved analysis. Search for $\nu_\mu \to \nu_e$ oscillation will be revised with about or more than twice statistics as the already published analysis [16]. Measurements of $\nu_\mu \to \nu_x$ oscillation parameters will be also updated, with more statistics and improved analysis technique.

6. Next Generation Experiment: T2K

Following the success of the first accelerator-based long baseline neutrino experiment K2K, the next generation long baseline experiment in Japan was planned. The new experiment, T2K (Tokai-to-Kamioka long baseline experiment) [17] will use high intensity proton beam from J-PARC (Japanese Proton Accelerator Research Complex), which is currently under construction at Tokai village in Japan. The far detector is SK, which will recover its original photo-coverage in 2006. The T2K experiment was approved in 2003 and the construction of the beamline was already started in 2004. The first beam is expected in 2009.

In order to maximize the sensitivity of the experiment, it is desired to tune the peak neutrino energy to the oscillation maximum while keeping high energy component, which is a dominant source of the background, as little as possible. T2K employs the off-axis beam configuration [18] to accomplish the highest possible intensity neutrino beam with a narrow energy spread. In the off-axis scheme, the beam axis is intentionally displaced by a few degrees from the far detector direction. With a finite decay angle, the neutrino energy becomes almost independent of the parent pion momentum, providing a narrow neutrino energy spectrum. The peak energy can be adjusted by changing the off axis angle. Using the world-highest power proton synchrotron at J-PARC, the expected neutrino flux in T2K is 50 times more of that in K2K.

The primary goals of T2K experiment are:

- Discovery of $\nu_\mu \to \nu_e$ oscillation and measurement of $\sin^2 2\theta_{13}$.
- Precision measurements of oscillation parameters Δm^2_{23} and $\sin^2 2\theta_{23}$ in ν_μ disappearance.
- Search for a sterile component in ν_μ disappearance by detecting neutral current events.

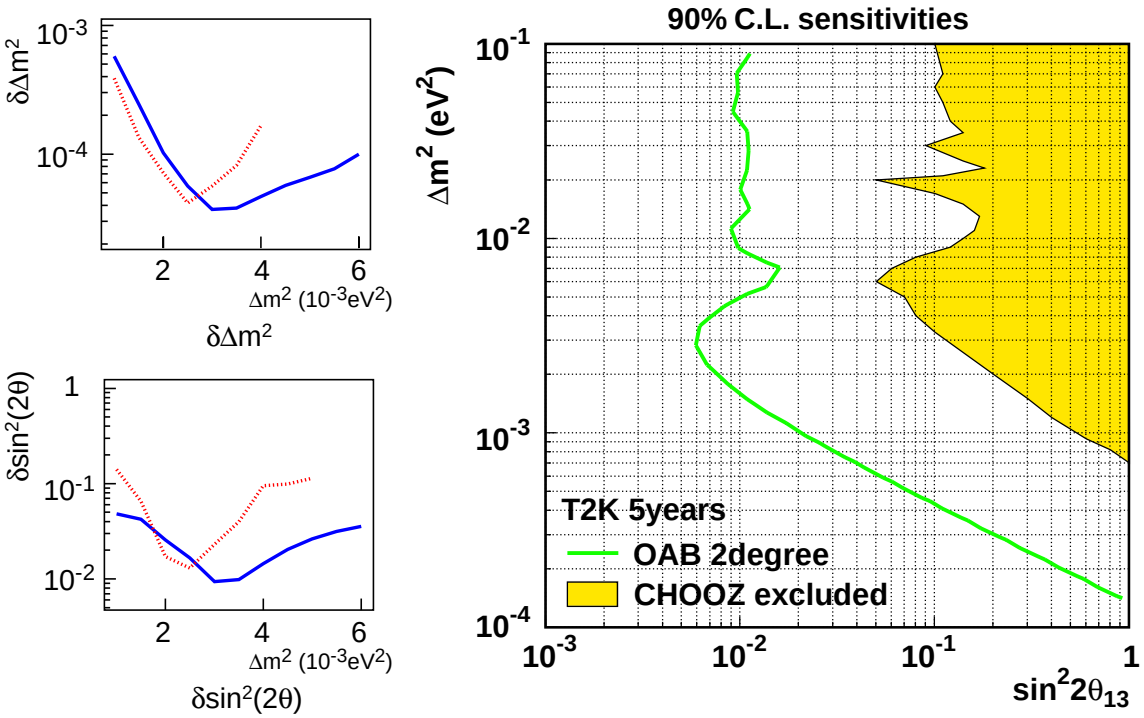

Figure 17: Expected sensitivities of T2K experiment after five years of operation with full intensity. Left: sensitivities for ν_μ disappearance parameters, Δm^2_{23}(top) and $\sin^2 2\theta_{23}$(bottom) as a function of true Δm^2_{23}. The $\sin^2 2\theta_{23}$ is set to 1.0. The results with off-axis angle 2 degree (3 degree) are shown by the solid (dashed) lines. Right: The 90% C.L. sensitivity for ν_e appearance with 2 degree off-axis angle. The 90% C.L. excluded region of CHOOZ [19] is also shown for comparison. $\sin^2\theta_{23}$ is assumed to be 0.5 and the possible contribution due to θ_{12} term is assumed to be small compared to the on due to θ_{13} term.

The expected sensitivities of ν_μ disappearance and ν_e appearance channels for five years of operation are shown in Fig. 17. For ν_μ disappearance, the error of Δm^2_{23} and $\sin^2 2\theta_{23}$ will be reduced down to 10^{-4} eV^2 and 0.01, respectively. Discovery of $\nu_\mu \to \nu_e$ oscillation will be possible for $\sin^2 2\theta_{13} > 0.006$, which provides a factor of twenty improvement over past measurements [19]. Once non-zero $\sin^2 2\theta_{13}$ is measured, study of CP violation in the lepton sector may be possible with $\nu_\mu \to \nu_e$ and its CP conjugate channel, $\overline{\nu}_\mu \to \overline{\nu}_e$. This would be a primary goal of the second stage of the T2K experiment with possible upgrade in the accelerator and the far detector.

7. Summary

The first accelerator-based long baseline neutrino oscillation experiment, K2K, has observed evidence for neutrino oscillation. Data taken from 1999 to 2004 are analyzed. A reduction of neutrino events and a distortion of neutrino energy spectrum, both are signatures of neutrino oscillation, were observed. The measurements are consistent with the neutrino oscillation, and the probability that we would see this result if there are no neutrino oscillations is 0.0050% (4.0σ).

The next generation long baseline neutrino oscillation experiment, T2K is being constructed, aiming for the startup of experiment in 2009. Using the high intensity proton beam and the off-axis configuration, T2K will significantly improve the sensitivity for neutrino oscillations in both ν_μ disappearance and ν_e appearance channels.

Acknowledgments

The author would like to thank the organizers of SSI04 for the kind invitation to such an excellent institute and for their great hospitality. He is grateful to all the collaborators of K2K experiment.

References

[1] S. H. Ahn *et al.* [K2K Collaboration], Phys. Lett. B **511**, 178 (2001); M. H. Ahn *et al.* [K2K Collaboration], Phys. Rev. Lett. **90**, 041801 (2003).
[2] Y. Fukuda *et al.* [Super-Kamiokande Collaboration], Phys. Rev. Lett. **81**, 1562 (1998); Y. Ashie *et al.* [Super-Kamiokande Collaboration], Phys. Rev. Lett. **93**, 101801 (2004).
[3] A. Suzuki *et al.* [K2K SciFi Group], Nucl. Instrum. Meth. A **453** 165 (2000); B. J. Kim *et al.*, Nucl. Instrum. Meth. A **497** 450 (2003).
[4] K. Nitta *et al.*, [K2K SciBar Group] Nucl. Instrum. Meth. A **535**, 147 (2004).
[5] T. Ishii *et al.* [K2K MRD Group], Nucl. Instrum. Meth. A **482**, 244 (2002) [Erratum-ibid. A **488**, 673 (2002)].
[6] D. Casper, these proceedings.
[7] S. Fukuda, *et al.* [Super-Kamiokande Collaboration], Nucl. Instrum. Meth. **A501**, 418-462 (2003).
[8] Y. Hayato, Nucl. Phys. Proc. Suppl. **112**, 171 (2002).
[9] C. H. Llewellyn Smith, Phys. Rept **3**, 261 (1972).
[10] D. Rein and L. M. Sehgal, Ann. Phys **133**, 79 (1981).
[11] D. Rein and L. M. Sehgal, Nucl. Phys. **B223**, 29 (1983).
[12] J. Marteau, J. Delorme and M. Ericson, Nucl. Instrum. Meth. **A451**, 76 (2000).
[13] M. Gluck, E. Reya and A. Vogt, Z. Phys. **C67**, 433 (1995).
[14] A. Bodek and U. K. Yang, Nucl. Phys. Proc. Suppl. **112**, 70 (2002).
[15] S. Nakayama *et al.* [K2K Collaboration], arXiv:hep-ex/0408134.
[16] M. H. Ahn *et al.* [K2K Collaboration], Phys. Rev. Lett. **93**, 051801 (2004).
[17] Letter of Intent for neutrino oscillation experiment at J-PARC, available from http://neutrino.kek.jp/jhfnu
[18] D. Beavis, A. Carroll, I. Chiang, *et al.*, Proposal of BNL AGS E-889 (1995).
[19] M. Apollonio *et al.* [CHOOZ Collaboration], Phys. Lett. B **466**, 415 (1999).